Abstract

We investigate the use of null space regularizing networks for linear ill-posed seismic inverse problems by combining a classic regularization method with the learned deep decomposition framework. This method extends the popular learned post-processing approach by learning how to improve an initial reconstruction with estimated missing components from the null space of the forward operator while naturally enforcing that the high-resolution prediction is always consistent with the low-resolution input. Unlike traditional model-based reconstruction algorithms, this approach does not make any prior explicit assumption on the solution. Employing a deep decomposition architecture, we consider the inversion of noisy data sets where an additional denoising component on the range of the pseudo-inverse is also trained. To illustrate the approach, we present two numerical examples: a single channel deconvolution and a tomographic (ray-based) inversion. By combining the classical regularization method of truncated singular value decomposition and the deep decomposition approach, we show that it is possible to achieve significant improvements upon the initial reconstruction.

Deep null space regularization for seismic inverse problems

Introduction

This paper considers the computation of an approximate solution for seismic inverse problems of the form

$$\mathbf{d}_\varepsilon = \mathbf{L}\mathbf{m} + \varepsilon, \tag{1}$$

where $\mathbf{L} : \mathbb{R}^n \rightarrow \mathbb{R}^m$ represents a linear forward operator that maps an earth model or unknown signal $\mathbf{m} \in \mathbb{R}^n$ to a data vector $\mathbf{d} \in \mathbb{R}^m$, and ε denotes an unknown data error (i.e., the noise). In this framework, most geophysical inverse problems are severely ill-posed due to a non-trivial null space of the forward operator. Therefore, many solutions fit the acquired data equally well, and a direct inversion $\mathbf{m}^* = \mathbf{L}^{-1}\mathbf{d}_\varepsilon$ to obtain the sought-after model is unattainable. Regularization techniques are generally implemented in traditional model-based methods to reduce null space ambiguity by imposing prior information to find a plausible solution. Although typical priors such as smoothness or sparsity constraints significantly improve the reconstruction quality, some details may still be lost, or artifacts remain in the solution. Furthermore, it can take a vast amount of time and effort to develop handcrafted formulations that fit a specific problem. Alternatively, data-driven methods based on deep neural networks can exploit detailed prior knowledge by learning it directly from existing data without human intervention.

Recently, several seismic applications have explored supervised techniques using Convolutional Neural Networks (CNNs), either as direct learned inversion (end-to-end) approaches (Araya-Polo et al., 2018; Mandelli et al., 2019), as learned iterative schemes (Torres and Sacchi, 2021), or as learned post-processing of an initial reconstruction (Kaur et al., 2020). Even though these methods have demonstrated remarkable empirical success, many supervised approaches still lack a data consistency restraint to enforce that the predicted model matches the acquired data, a necessary condition for a reliable solution to the inverse problem. Hence, the results might look realistic, but there is no way to assess their accuracy. Unsupervised approaches (Zhang et al., 2021; Kong et al., 2022) address this issue by design, but they often amplify the expensive iterative nature of traditional methods when the trainable weights are not correctly initialized.

Regularization via null space networks (Schwab et al., 2019) has been introduced as an alternative to the learned post-processing method to account for data consistency. By computing a projection onto the null space of the forward operator after the last weight layer of a residual architecture, it is possible to train a neural network to learn the missing components of the initial reconstruction given by the pseudoinverse $\mathbf{L}^\dagger : \mathbb{R}^m \rightarrow \mathbb{R}^n$ (or an approximation to it). As a generalization to null space networks, Chen and Davies (2020) introduced the concept of deep decomposition learning, which attaches a complementary network to act as a denoiser on the range of the pseudoinverse. Based on this idea, we investigate the extension of deep null space learning on two seismic inverse problems, namely, a single channel deconvolution example and a tomographic (ray-based) crosswell inversion. Specifically, we extend the deep decomposition approach by using the truncated singular value decomposition (TSVD) as an initial regularized reconstruction for approximating the low-frequency components of the model. In a second step, we trained two neural networks to recover the missing parts of the model and the "inverted" noise, respectively.

Method

We can decompose the domain of the forward operator into two sub-spaces: the measurement space and the null space. Accordingly, we might think of any model $\mathbf{m}$ in the domain of $\mathbf{L}$ as being made up of two unique orthogonal vectors,

$$\mathbf{m} = \mathbf{m}_R + \mathbf{m}_N = P_R(\mathbf{m}) + P_N(\mathbf{m}), \tag{2}$$

such that $\mathbf{m}_R$ lies in the range of the pseudoinverse $\mathbf{L}^\dagger$, and $\mathbf{m}_N$ lies in the null space. By definition, these two components satisfy, respectively,

$$\mathbf{m}_R = \mathbf{L}^\dagger \mathbf{d}_\varepsilon = \mathbf{L}^\dagger \mathbf{L}\mathbf{m} + \mathbf{L}^\dagger \varepsilon, \tag{3}$$

and

$$\mathbf{L}\mathbf{m}_N = 0. \tag{4}$$

Based on this fragmentation of the model, we can express the ideal reconstruction as

$$\mathbf{m}^* = \mathbf{L}^\dagger \mathbf{d}_\varepsilon - \mathbf{L}^\dagger \varepsilon + \mathbf{m}_N. \tag{5}$$

In other words, the solution is expressed in terms of a unique minimum norm least-squares solution ($\mathbf{L}^\dagger \mathbf{d}_\varepsilon$) minus the "inverted" noise plus the null space vector.

As denoted in equation 2, the model components can be obtained from two orthogonal projections, P_R and P_N, defined as

$$P_R = \mathbf{L}^\dagger \mathbf{L}, \tag{6}$$

and

$$P_N = \mathbf{I} - \mathbf{L}^\dagger \mathbf{L}, \tag{7}$$

where $\mathbf{I} \in \mathbb{R}^n$ is the identity operator. Using a physics-engaged approach promoted by the application of the above-mentioned orthogonal projections, deep decomposition learning attempts to solve equation 5 with a trained estimator $\Lambda : \mathbb{R}^m \rightarrow \mathbb{R}^n$ defined as

$$\Lambda(\mathbf{d}_\varepsilon; \theta_1, \theta_2) = \mathbf{L}^\dagger \mathbf{d}_\varepsilon + P_R \circ \mathbf{F}_{\theta_1} \circ \mathbf{L}^\dagger \mathbf{d}_\varepsilon + P_N \circ \mathbf{N}_{\theta_2} \circ (\mathbf{L}^\dagger \mathbf{d}_\varepsilon + P_R \circ \mathbf{F}_{\theta_1} \circ \mathbf{L}^\dagger \mathbf{d}_\varepsilon), \tag{8}$$

where $\mathbf{F}_{\theta_1}$ and $\mathbf{N}_{\theta_2}$ are two trainable neural networks. Compared to equation 5, it is clear that the second term in equation 8 tries to estimate the negative "inverted" noise by projecting the output of the network $\mathbf{F}_{\theta_1}$ onto the range of the pseudoinverse. Likewise, the third term in equation 8 tries to estimate the null space component from the denoised input $\mathbf{L}^\dagger \mathbf{d}_\varepsilon + P_R \circ \mathbf{F}_{\theta_1} \circ \mathbf{L}^\dagger \mathbf{d}_\varepsilon \approx \mathbf{L}^\dagger \mathbf{d}_\varepsilon - \mathbf{L}^\dagger \varepsilon$. When Λ lacks the explicit denoising element ($P_R \circ \mathbf{F}_{\theta_1} \circ \mathbf{L}^\dagger \mathbf{d}_\varepsilon = 0$), the estimator turns into a standard null space regularization network of the form

$$\Lambda(\mathbf{d}_\varepsilon; \theta) = \mathbf{L}^\dagger \mathbf{d}_\varepsilon + P_N \circ \mathbf{N}_\theta \circ \mathbf{L}^\dagger \mathbf{d}_\varepsilon, \tag{9}$$

$$\Lambda(\mathbf{d}_\varepsilon; \theta) = (\mathbf{I} + P_N \circ \mathbf{N}_\theta)(\mathbf{L}^\dagger \mathbf{d}_\varepsilon), \tag{10}$$

where the data consistency property, $\mathbf{L}\Lambda(\mathbf{d}_\varepsilon; \theta) = \mathbf{d}_\varepsilon$ is preserved.

In the following section, we use the TSVD for computing a regularized approximation $\mathbf{L}_k^\dagger$ to the exact pseudoinverse, where the regularization parameter $k > 0$ designates the number of non-truncated singular values and is chosen such that that $\mathbf{m}^*_{\text{TSVD}} = \mathbf{L}_k^\dagger \mathbf{d}_\varepsilon$ has the minimal l_2 difference to the true model. By only recovering signal components corresponding to sufficiently large singular values, TSVD produces a stable solution that prevents small singular values of $\mathbf{L}$ to amplify noise. On the other hand, the absent components have an unreliable model-to-data mapping and therefore will be recovered in the learning stage. We stress that we only need to compute the TSVD of $\mathbf{L}$ once before training for a specific acquisition setup. Finally, the overall procedure aims to jointly seek

$$\arg\min_{\theta_1, \theta_2} \frac{1}{N} \sum_{i=1}^{N} ||\mathbf{m}^i - \Lambda(\mathbf{d}^i_\varepsilon; \theta_1, \theta_2)||_2^2 + \lambda_1 \sum_{i=1}^{N} ||\mathbf{L}\mathbf{F}_{\theta_1}(\mathbf{L}_k^\dagger \mathbf{d}^i_\varepsilon) - \varepsilon^i||_2^2 + \lambda_2 ||\theta_2||_2^2, \tag{11}$$

where the first term carries out the supervised training on a synthetic dataset $\mathscr{D} = \{(\mathbf{m}^i, \mathbf{d}^i_\varepsilon)\}_{i=1}^N$ using the MSE loss, the second term prevents the denoising component from breaking the data consistency property, and the third term provides the null space estimator with robustness to small perturbations via weight regularization (Schwab et al., 2019). In this work, we define $\mathbf{F}_{\theta_1} = \sigma_4 \circ \mathbf{W}_4 \circ ... \circ \sigma_1 \mathbf{W}_1$ as a four-layered CNN denoising network where σ_i represents the ReLU function, and $\mathbf{W}_i$ is a matrix with trainable weights. We set $\mathbf{N}_{\theta_2}$ as the original U-net architecture.

Numerical Examples

We evaluate the learned regularization method described in the previous section on two different seismic inverse problems that can be synthesized using equation 1: a simple 1D deconvolution example and a 2D crosswell (ray-based) tomography. Setting the trade-off parameters $\lambda_1 = 10e^{-6}$ and $\lambda_2 = 10e^{-8}$ yields stable solutions for the two applications considered. In both experiments, we incorporate different realizations of additive Gaussian noise to the clean data such that the signal-to-noise ratio is equal to 20%. In all cases, equation 11 was minimized using stochastic gradient descent with 400 epochs and a learning rate of 0.001.

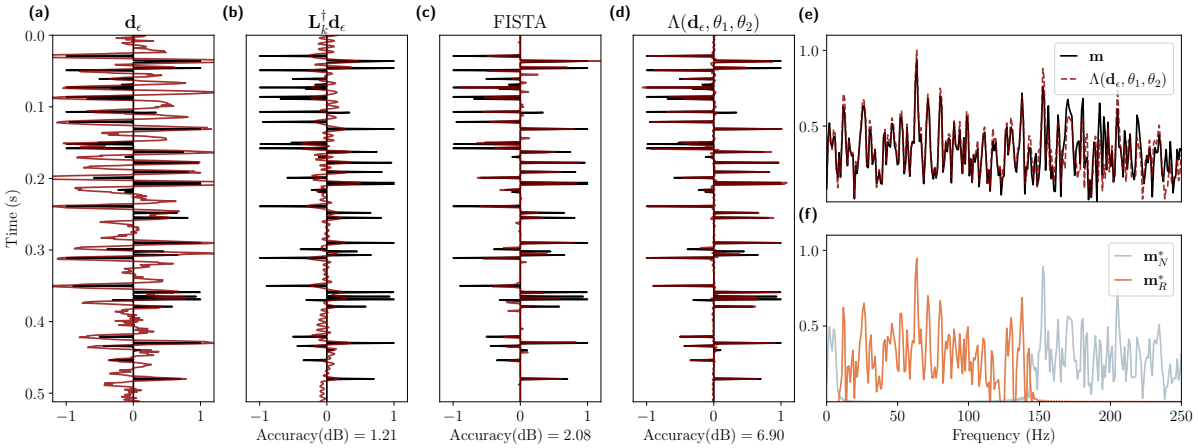

Figure 1 *Deconvolution example. True reflectivity* $\mathbf{m}$ *superposed with (a) the noisy trace* $\mathbf{d}_\varepsilon$*, (b) the TSVD result, (c) the FISTA result, and (d) the deep null space regularization. Figure (e) compares the amplitude spectrum of the true reflectivity model and the deep null space regularization solution, and Figure (f) shows the amplitude spectrum of the individual range (orange) and null space (gray) retrieved components.*

Deconvolution

Relying on the convolutional model of the seismic trace, we attempt to recover a full-band reflectivity sequence from a zero-offset trace. The forward operator represents a band-limited wavelet matrix expressing time-invariant convolution in this example. To train the estimator, we randomly generate 5000 reflectivity samples and obtain the corresponding data by convolving a 60 Hz Ricker wavelet and adding the random noise. Figure 1 shows the results for a test reflectivity model different from all training samples but generated using the same random procedure. For a quantitative evaluation of the results, we calculate the reconstruction accuracy (dB) $= 10 \times \log_{10} ||\mathbf{m}||_2^2 / ||\mathbf{m} - \mathbf{m}^*||_2^2$, where $\mathbf{m}$ and $\mathbf{m}^*$ are the true and inverted reflectivity models, respectively. Figure 1b shows the initial TSVD solution, where some of the most prominent reflections are partially recovered, but a residual band-limited component masks the non-resolvable events. Moreover, oscillations are visible in the result due to the truncated expansion. For comparison, Figure 1c displays a sparse-spike deconvolution result obtained with 100 iterations of the FISTA solver. Even though the inversion with sparsity promotion enables a full-band solution, the noisy data impedes successfully retrieving the correct amplitude and positioning of some events. Figure 1d shows the result obtained with deep null space regularization, where we conclude that, both visually and quantitatively, the learned estimator inversion produces higher quality results compared to the two previous techniques. Finally, Figures 1e and 1f show the amplitude spectrum of the true and the estimated result and the amplitude spectrum of the solution's range and null space components. Both figures show that deep null space regularization approximately recovers the missing frequency components of the original signal.

Linearized traveltime tomography

The second test entails a straight ray tomographic inversion, where we seek a velocity model $\mathbf{m}$ parameterized by the slowness from noisy traveltime measurements $\mathbf{d}_\varepsilon$ by approximately inverting the tomographic matrix $\mathbf{L}$, which contains the segment lengths of the rays. The acquisition setup describes a 2D transmission experiment where 128 sources and 128 receivers are evenly distributed along the right and left boundaries of a discretized 128×128 grid cell domain. We generate the training data as in Torres and Sacchi (2021) using 1000 folded and fractured pseudo-random velocity models. Additionally, we include salt bodies in 250 training models, where the position, size, and shape of the salt anomalies are randomly chosen. We examine the method's performance on a test model that was not used during training and has a salt body on the lower part of the domain (Figure 2a). Figure 2b displays the initial reconstruction given by the TSVD, where the best-resolved features are the nearly horizontal sedimentary layers with velocity gradients perpendicular to the rays. However, we observe mismatches in the

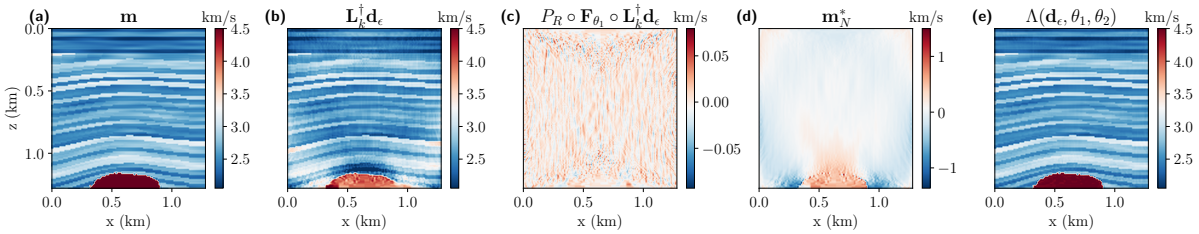

Figure 2 *Crosswell tomography inversion. (a) the true velocity model, (b) the TSVD result, (c) the predicted inverted noise component, (d) the null space prediction, (e) the output of the learned estimator.*

estimated velocities and a resolution reduction at the deeper part near the salt body. In contrast, Figure 2e shows the output of the learned estimator, which improves upon the initial regularized solution. In addition, Figures 2d and 2e show the inverted noise component and the null space component predicted by the two projections, respectively. We can see that there is no coherent signal in the inverted noise component. Furthermore, the null space component accurately recovers the missing parts of the model around the salt body.

Conclusions

In this work, we investigated the use of regularizing networks via the deep decomposition approach to solve two ill-posed seismic inverse problems. We illustrate how learned null space regularization adds reasonable estimates from the null space, improving classic regularization solutions. Additionally, we combined the deep decomposition learning method with TSVD, which helps produce clean inputs for the efficient training of the null space network. An important research direction is to identify ways of efficiently integrating deep null space regularization with bigger problems where the direct computation of the orthogonal projections is prohibitively expensive.

Acknowledgements

The research leading to this paper was supported by the Signal Analysis and Imaging Group (SAIG) sponsors at the University of Alberta. We thank Dongdong Chen for providing the implementation of the deep decomposition architecture.

References

Araya-Polo, M., Jennings, J., Adler, A. and Dahlke, T. [2018] Deep-learning tomography. *The Leading Edge*, **37**(1), 58–66.

Chen, D. and Davies, M. [2020] Deep Decomposition Learning for Inverse Imaging Problems. 1–17. Technical report; null ; Conference date: 23-08-2020 Through 28-08-2020.

Kaur, H., Pham, N. and Fomel, S. [2020] Improving the resolution of migrated images by approximating the inverse Hessian using deep learning. *GEOPHYSICS*, **85**(4), WA173–WA183.

Kong, F., Picetti, F., Lipari, V., Bestagini, P., Tang, X. and Tubaro, S. [2022] Deep Prior-Based Unsupervised Reconstruction of Irregularly Sampled Seismic Data. *IEEE Geoscience and Remote Sensing Letters*, **19**, 1–5.

Mandelli, S., Borra, F., Lipari, V., Bestagini, P., Sarti, A. and Tubaro, S. [2019] Seismic data interpolation through convolutional autoencoder. *2018 SEG International Exposition and Annual Meeting, SEG 2018*, 4101–4105.

Schwab, J., Antholzer, S. and Haltmeier, M. [2019] Deep null space learning for inverse problems: Convergence analysis and rates. *Inverse Problems*, **35**(2).

Torres, K. and Sacchi, M. [2021] Deep learning based least-squares reverse-time migration. *First International Meeting for Applied Geoscience & Energy Expanded Abstracts*, 2709–2713.

Zhang, W., Gao, J., Jiang, X. and Sun, W. [2021] Consistent Least-Squares Reverse Time Migration Using Convolutional Neural Networks. *IEEE Transactions on Geoscience and Remote Sensing*, 1–18.